

GROWTH, STRUCTURAL, OPTICAL, MECHANICAL AND DIELECTRIC PROPERTIES OF GLYCINE SODIUM NITRATE (GSN) SINGLE CRYSTAL

S. SURESH^{a*}, A. RAMANAND^a, P. MANI^b, KALIYA MURTHYANAND^c

^a*Department of Physics, Loyola College, Chennai – 600 034, India*

^b*Department of Physics, Hindustan University, Padur, India*

^c*Department of Physics, Manakulavinayagar Institute of technology, Pondicherry, India*

The Single crystals of Glycine Sodium Nitrate (GSN) with very high degree of transparency were grown from aqueous solution by slow evaporation technique. Single crystal X-ray diffraction analysis reveals that the crystal belongs to monoclinic system with the space group Cc. The density measurements were carried out by both theoretical and experimental methods. The optical absorption study reveals the transparency of the crystal in the entire visible region and the cut off wavelength was found to be 310 nm. The dependence of extinction coefficient (k) and refractive index (n) on the absorption has also been reported. The refractive index was measured by the Brewster's angle method. The Non Linear Optical (NLO) behaviour of GSN crystals was tested by Kurtz- Powder technique. The mechanical hardness was studied by Vickers microhardness tester. The Dielectric studies were also reported as a function of frequency at room temperature. The photoconductivity reveals the negative nature of the photocurrent in these crystals.

(Received July 19, 2010; accepted July 23, 2010)

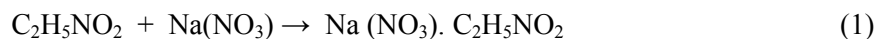
Keywords: Growth from solutions, Dielectric, Mechanical properties

1. Introduction

Among the organic materials amino acids constitute a family in which glycine is the simplest of all the aminoacids. It has been reported that some complexes of amino acids with simple inorganic salts may exhibit ferroelectric properties (1-4). Some complexes of glycine (5-10) form single crystals but none of these are reported to have nonlinear optical property. In the present investigation, the growth aspects of the Glycine Sodium Nitrate (GSN) crystal have been carried out in isothermal solvent evaporation technique. The grown crystal is subjected to characterization such as single X-ray analysis, optical analysis, mechanical hardness, and dielectric, SEM, and Photoconductivity studies in detail.

2. Experimental

Single crystals of GSN were grown, from aqueous solution by slow evaporation technique. The starting materials were analytical grade reagents glycine and sodium nitrate. The solution was prepared by dissolving equimolar amounts of glycine and sodium nitrate in deionized water by slow evaporation at ambient temperature according to the equation



Small transparent seed crystals were obtained through spontaneous nucleation. Single crystals were grown to a dimension of 22 x 20 x 10 mm³ as shown in Fig. 1. During the growth of GSN fungus like organism were formed in the solution. These organisms initially start on the

surface and gradually after a few days sink into the solution thereby, contaminating it and growth of the crystals to larger dimension is prohibited. The growth of these microbes is prevented by adding a few drops of hydrogen peroxide (H_2O_2).

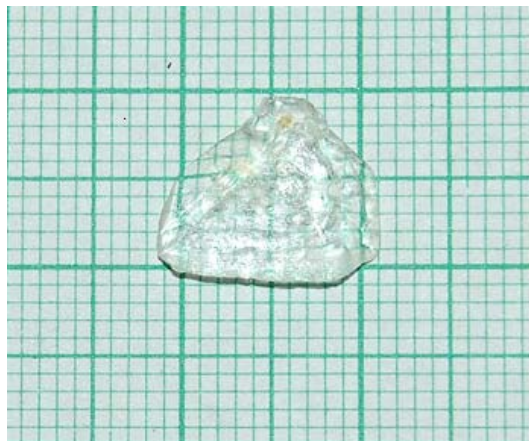


Fig. 1. Grown single crystals of GSN

3. Results and discussion

Single crystal XRD

The single crystal X-ray diffraction (XRD) analysis for the grown crystals has been carried out to identify the lattice parameter which is confirmed from the structure shown in Fig 2. The calculated lattice parameters are $a=14.323 \text{ \AA}$, $b=5.2573 \text{ \AA}$, $c=9.1156 \text{ \AA}$ and the crystal belongs to monoclinic system with space group Cc (11)

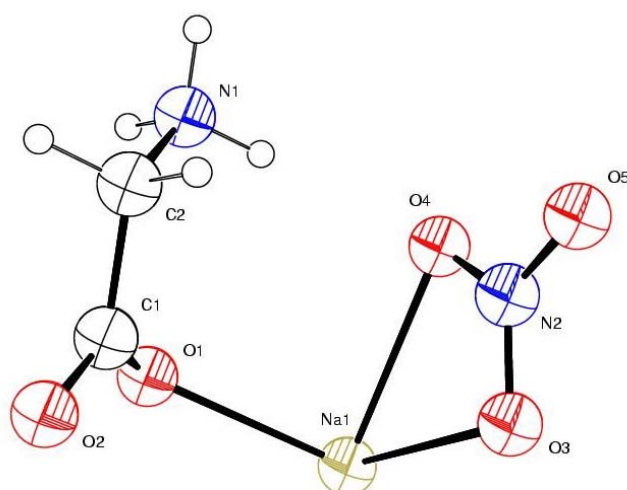


Fig.2. ORTEP representation of GSN crystal molecules with atom numbering scheme.

Density measurements

The density of GSN crystal was calculated by the equation shown below (12)

$$\rho = MZ / N_A abc \quad (2)$$

Where M is molecular weight of GSN; Molecular Unit cell $Z = 4$; N_A is Avogadro's number and a , b and c are the lattice parameters of GSN crystal. The theoretical density is found to be 1.7691 g/cm^3 . The density of GSN crystal was measured experimentally by the floatation method at room temperature (32°C), and the measured density can be obtained by the following equation

$$\rho = M \rho_{\text{solvent}} / m - m' \quad (3)$$

Where m is the mass of GSN crystal sample in the air, m' is the mass when the GSN crystal sample was immersed in CCl_4 and ρ_{solvent} is the density of solvent (CCl_4) used at measured temperature. The density was measured by floatation technique. From this measurement, the density of the crystal is found to be 1.7690 g/cm^3 . The experimentally measured density is in good agreement with the theoretically found values.

Optical absorption studies

The optical absorption spectrum of Glycine Sodium Nitrate (GSN) single crystal was recorded in the wavelength region ranging from 200 nm to 2000nm using a Varian Cary 5E spectrophotometer and is shown in Fig 3. For optical fabrications, the crystal should be highly transparent in a considerable region of wavelength (13,14). The UV cut off wavelength for the grown crystal was found to be 310 nm which makes it a potential material for optical device fabrication.

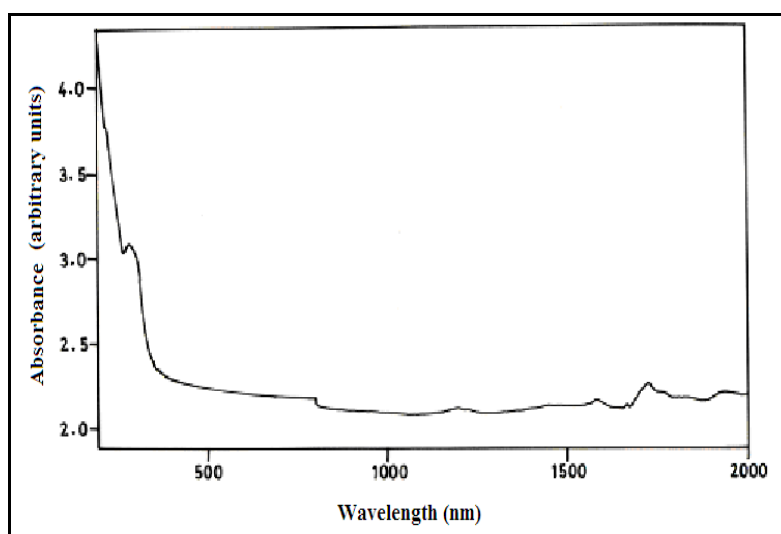


Fig 3. Optical absorption spectrum of GSN single crystal

$$\alpha = \frac{1}{d} \log \left(\frac{1}{T} \right) \quad (4)$$

Where T is the transmittance and d is the thickness of the crystal. As a direct band gap material, the crystal under study has an absorption coefficient (α) obeying the following relation for high photon energies ($h\nu$)

$$\alpha = \frac{A(h\nu - E_g)^{1/2}}{h\nu} \quad (5)$$

Where E_g in the optical band gap of the crystal and A is a constant. The plot of variation of $(\alpha h\nu)^2$ versus $h\nu$ is shown in Fig. 4. E_g was evaluated by the extrapolation of the linear part (15). The band gap is found to be 4.0 eV, as a consequence of wide band gap, the grown crystal has large transmittance in the visible region (16).

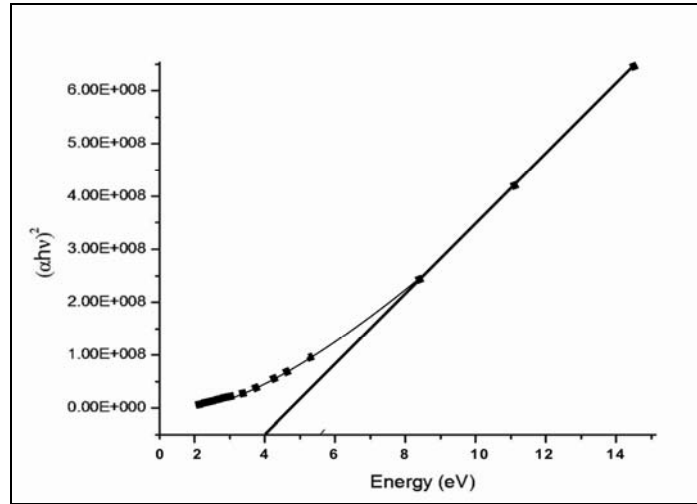


Fig. 4. Plot of α versus photon energy for GSN single crystals

Determination of optical constants

The optical constant (n, k) are determined from the transmission (T) and reflection (R) spectrum based on the following relations (17)

$$T = \frac{(1-R)^2 \exp(-\alpha t)}{1-R^2 \exp(-2\alpha t)} \quad (6)$$

Where t is the thickness and α is related to extinction coefficient k by

$$K = \frac{\alpha \lambda}{4\pi} \quad (7)$$

The refractive index (n) can be determined from the reflectance (R) data using the relation (18)

$$R = \frac{(n-1)^2}{(n+1)^2} \quad (8)$$

Where R the reflectance in terms of absorption coefficient can be written

$$R = \frac{1 \pm \sqrt{1 - \exp(-\alpha t) + \exp(\alpha t)}}{1 + \exp(-\alpha t)} \quad (9)$$

From the above equation, the refractive index n can also be derived as

$$n = -\frac{(R+1) \pm \sqrt{3R^2 + 10R - 3}}{2(R-1)} \quad (10)$$

Figs. 5 and 6 show the variation of Extinction coefficient (K) and Reflectance (R) as a function of absorption respectively. From the graphs, it is clear that both the reflectance and extinction coefficient depend on the wavelength. Since the internal efficiency of the device also depends on the wavelength, by tailoring the wavelength one can achieve the desired material to fabricate the optoelectronic devices.

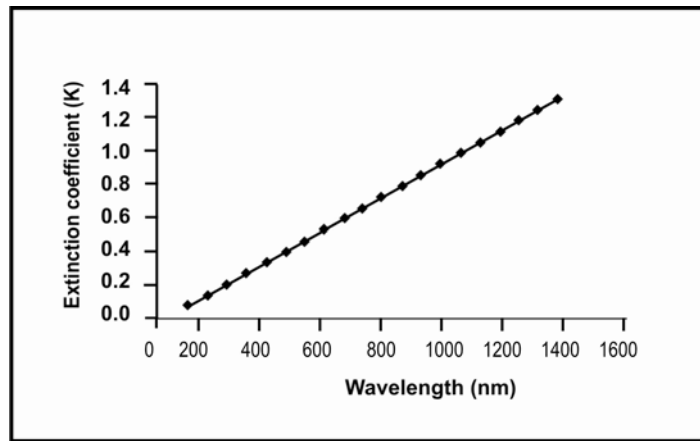


Fig. 5. Plot of wavelength versus extinction coefficient (k).

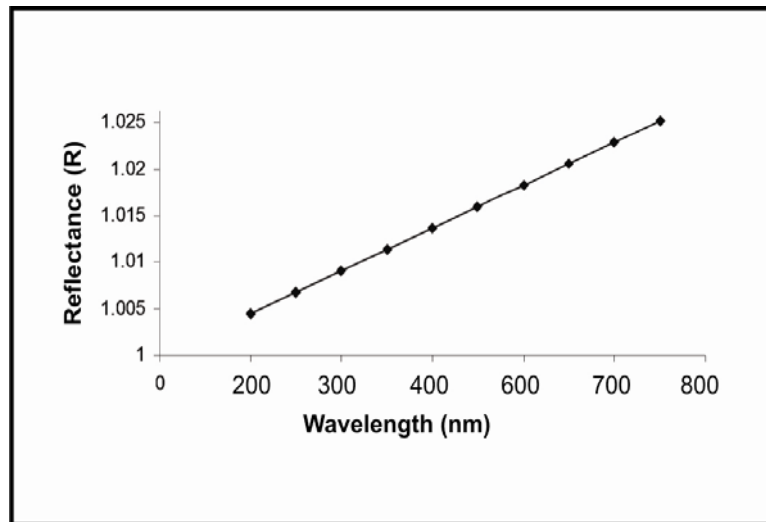


Fig. 6. Plot of wavelength versus reflectance (R).

Refractive index (n) measurement

The refractive index of the GSN crystal was determined by Brewster's angle method using He-Ne laser of wavelength 632.8 nm. A polished flattened single crystal of GSN was mounted on a rotating mount at an angle varied from 0 to 90 degrees. The angular reading on the rotary stage was observed, when the crystal is perfectly perpendicular to the intra-cavity beam. The crystal was

rotated until the laser oscillates and the angle has been set for maximum power output. Brewster's angle (θ_p) for GSN is measured to be 56.50 ± 0.5 degree. The refractive index has been calculated using the equation

$$n = \tan\theta_p \quad (11)$$

Where θ_p is the polarizing angle and n is found to be 1.510.

SEM analysis

The surface morphology and dislocation on the surface of the grown crystal along (001) was magnified using a JSM 840-A scanning electron microscope. The transparent growth plane of the GSN crystal was coated with gold to discharge the charge of particles and scanned magnification. The image part of the crystal surface of glycine sodium nitrate as shown in Fig. 7 is free from dislocation network and visible inclusion, yet a small crack of length of about $10 \mu\text{m}$ was observed on the surface of the crystal. This confirms the perfection of the grow crystal.

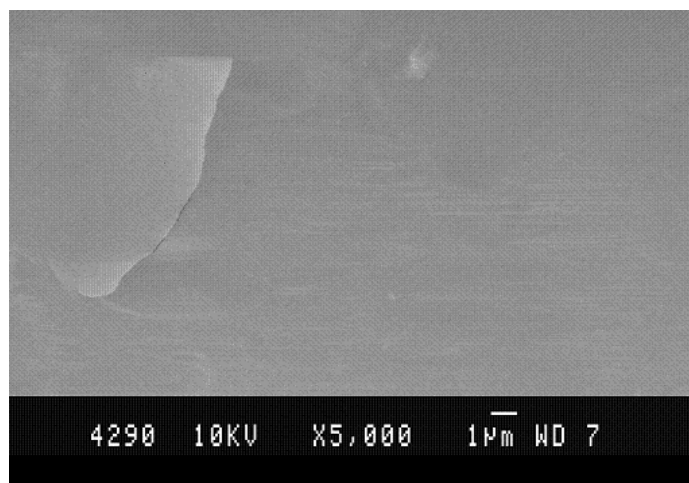


Fig. 7. SEM Photograph of GSN single crystal

Dielectric studies

The dielectric study GSN single crystal was carried out using the instrument, HIOKI 3532-50 LCR HITESTER. A sample of dimension $7.52 \times 5.62 \times 1.35 \text{ mm}^3$ having silver coating on the opposite faces was placed between the two copper electrodes and thus a parallel plate capacitor was formed. The capacitance of the sample was measured by varying the frequency from 50 Hz to 5 MHz. Fig.8 shows the plot of dielectric constant (ϵ_r) versus applied frequency. The dielectric constant is high in the lower frequency region (50 Hz) and then it decreases with the applied frequency. The dielectric constant is 319.47 at 50 Hz and decreases to 97.2 at 30 kHz. The very high value of ϵ_r at low frequencies may be due to the presence of all the four polarizations namely space, charge, orientational, electronic and ionic polarization and its low value at higher frequencies may be due to the loss of polarizations gradually. The dielectric loss is also studied as a function of frequency at room temperature and is shown in Fig.9. These curves suggest that the dielectric loss is strongly dependent on the frequency of the applied field, similar to that of dielectric constant. This behaviour is common in the case of ionic systems (19, 20).

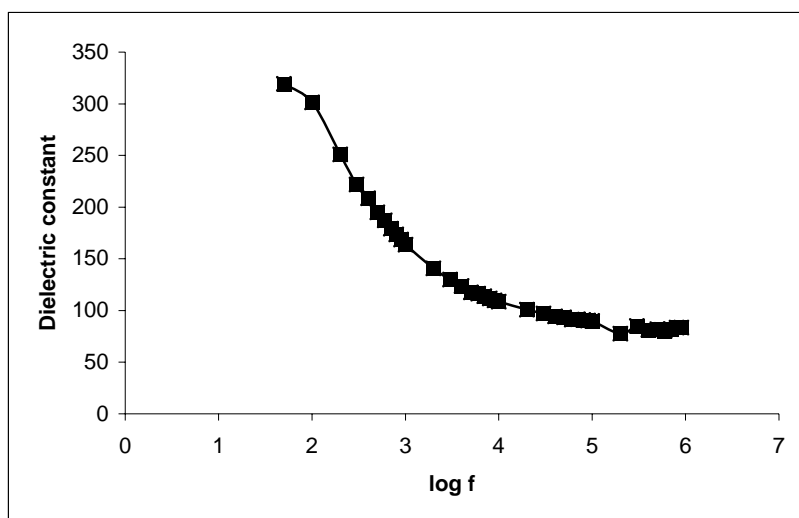


Fig. 8. Variation of dielectric constant vs frequency.

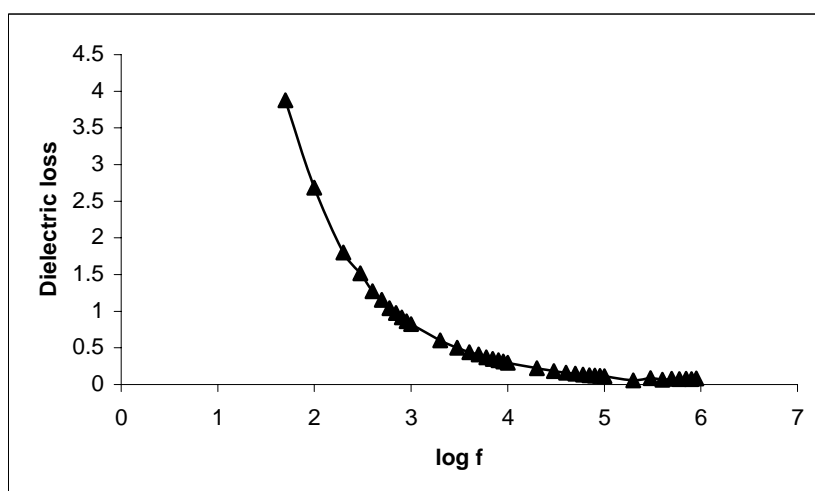


Fig. 9. Variation of dielectric loss vs frequency

Photoconductivity studies

The photoconductivity studies of grown crystals were carried out by connecting the sample in series with a dc powder supply and a Pico ammeter (Keithley 480) at room temperature. The setup is similar to that in the work of Ledorux (21). The applied field was increased from 100 to 1800 V/cm, and the corresponding dark current and photocurrent were recorded. Fig. 10 shows the dependence of the dark current and photocurrent with respect to the applied field at room temperature. The dark current and photocurrent increase linearly with respect to the applied field. At every instant, the dark current is greater than the photocurrent, which is called negative photoconductivity. This may be attributed due to decrease in either the number of free charge carriers or their lifetime when subjected to radiation. According to the Stockmann model, the forbidden gap in the material contains two energy levels in which one is situated between the Fermi level and the conduction band while the other is located close to the valence band (22) the second state has high capture cross sections for electrons and holes. As it captures electrons from the conduction band and holes from the valence band, the number of charge carriers in the

conduction bands gets reduced and the current decreases in the presence of radiation. Thus the crystal is said to exhibit negative photo conducting effect.

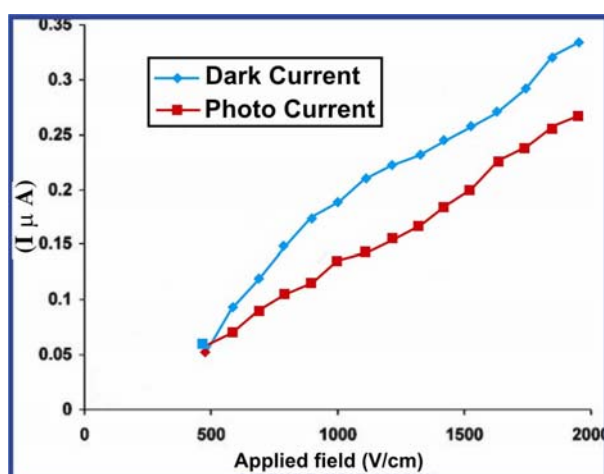


Fig.10. Dark current and photocurrent as a function of the applied field.

Mechanical properties

The mechanical characterization of grown crystals was made by Vickers Microhardness tests at room temperature. Single flat crystal with polish surfaces free from cracks was chosen for the static indentation tests. The surface (0 1 2) was polished gently with water before measurements. The crystal was mounted properly on the base of the microscope. Now the selected faces was indented gently by the loads varying from 10 to 50 g for a dwell period of 10 sec using both Vickers diamond pyramid indenter and Knoop indenter attached to an incident ray research microscope (Mututoyo MH 112, Japan). The Vickers indented impressions were approximately square in shape. The shape of the impression is structure dependent, face dependent and also material dependent. For a particular load, at least five well-defined impressions were considered and the average of all the diagonals (d) was considered. The Vickers hardness number (H_v) was calculated using the standard formula:

$$H_v = 1.8544 P / d^2, \quad (12)$$

Where P is the applied load in kg, d in mm and H_v is in kg/mm^3 .

Crack initiation and materials chipping become significant beyond 50 g of the applied load. So hardness test could not be carried out above this load. It reveals that the density of defects in the crystal is the form of vacancy (23) Increasing non-Centro symmetry due to the presence of an enhanced number of vacancies may be physical origin of the observed phenomenon. A Crystal defect purely depends on the crystal growth condition.

The elastic stiffness constant (c_{11}) is expressed by Wooster's empirical relation as $c_{11} = H^{7/4}$ (24). As indentation initiates plastic deformation in a crystal, which is highly directional in nature, the hardness measurement may be a function of the orientation of the indented crystal. Figure 11 shows the variation of H_v as a function of applied load ranging from 10 g to 50 g on (0 1 2) face for GSN crystal. It is very clear from the figure that H_v increases with increase of load.

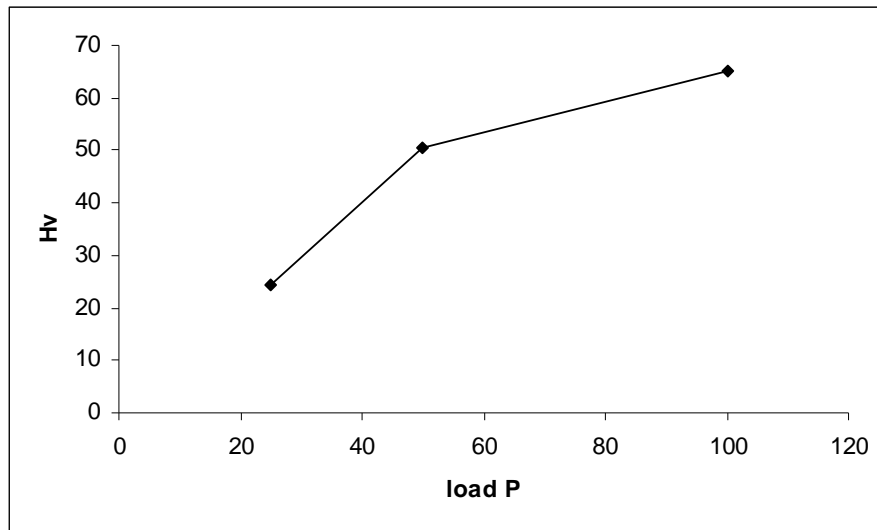


Fig. 11. Load P vs hardness H_v

The Meyer's index number was calculated from the Meyer's law, which relates the load and indentation diagonal length. $P = k d^n$, $\log P = \log k + n \log d$, where k is the material constant and n is the Meyer index. In order to calculate the value of 'n', the graph is plotted against $\log P$ versus $\log d$ shown in figure 12, which gives a straight line; the slope of this straight line gives the value of 'n'. The calculated value of 'n' is 2.1, from the expression $H_v = b P^{(n-2)/n}$. H_v should increase with increase of P if $n > 2$ and decrease with same if $n < 2$. The 'n' value agrees well with the experiment. Conducted by Onitsch (25, 26). 'n' should lie between 1 to 1.6 for harder materials and above 1.6 for softer materials. Thus GSN belongs to the soft material category.

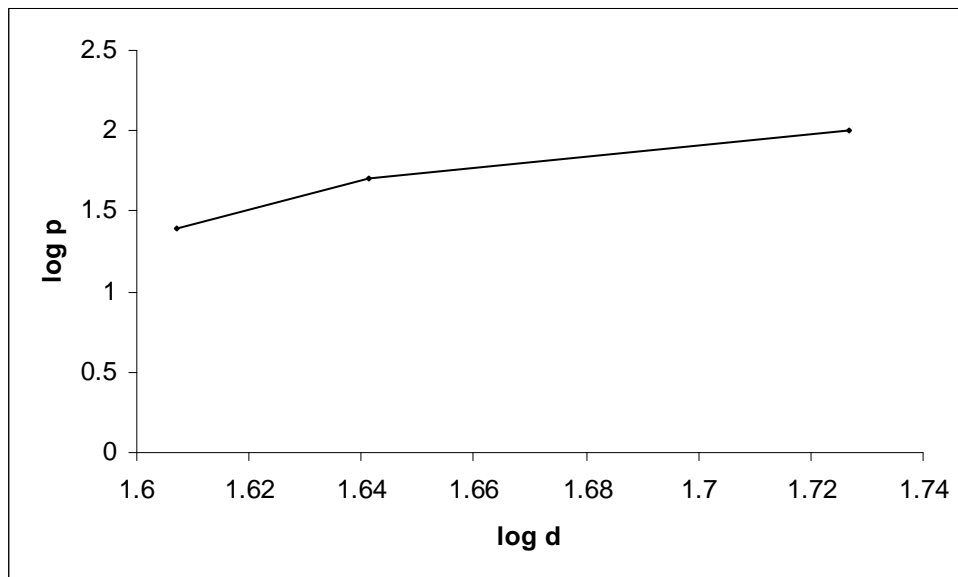


Fig. 12. $\log P$ vs $\log d$

The resistance pressure is defined as a minimum level of indentation load (W) below which there is no plastic deformation. Hays and Kendall proposed a relationship to calculate 'W' by the equation

$$d^n = W/k_1 + (k_2 / k_1) d^2. \quad (13)$$

The plot between d^n and d^2 figure gives a straight line having slope k_2/k_1 and intercepts W/k_1 . From these values the value of W was calculated as 7.18g and the value of n was 4.75.

The calculated stiffness constant for different loads is shown in Table 1. The elastic stiffness constant (c_{11}) was calculated by using Wooster's empirical relation.

Table 1 Stiffness constant of GSN

H_v (kg/mm ³)	C_{11}
24.3	265.956
50.65	961.643
65.20	1496.005

NLO studies

Kurtz second harmonic generation (SHG) test was performed to find the NLO property of GSN crystal. The crystal was illuminated using Spectra Physics Quanta Ray DHS2. Nd: YAG laser using the first harmonic output of 1064 nm with pulse width of 8 ns and repetition rate 10 Hz. The second harmonic signal, generated in the crystal was confirmed from the emission of green radiation by the crystal. The SHG radiation of 532 nm green light were collected by a photo multiplier tube (PMT-Philips Photonics — model 8563) after being monochromated (monochromator — model Triax-550) to collect only the 532 nm radiations. The optical signal incident on the PMT was converted into voltage output at the CRO (Tektronix-TDS 3052B). The input laser energy incident on the powdered sample was chosen to be 3.4 mJ. The result obtained for GSN shows a powder SHG efficiency of about 2 times that of KDP crystal.

4. Conclusions

Transparent single crystals of GSN have been grown successfully using slow solvent evaporation technique. X-ray analysis reveals that GSN crystallizes into the monoclinic system with space group Cc. The density of GSN crystals is found to be 1.7690 g/cm³ which are in accordance with theoretical calculations. UV - Visible absorption spectrum shows excellent transmission in the entire visible region. The band gap energy for the grown crystal is found to be 4.0 eV. The optical investigations show a high value of both extinction coefficient (k) and reflectivity (R) indicating high transparency of the crystal which confirms its suitability for optical device fabrication. The dielectric studies were studied as a function of frequency. The dielectric study shows low dielectric loss behaviour, signifying that the grown crystal is relatively defecting free. Photoconductivity studies confirm that the crystal possesses a negative photoconducting nature. SEM study reveals crystal morphology and surface perfection of the grown crystal. The variation of Vickers hardness number (H_v) as a function of applied load on (0 1 2) plane shows that H_v increases with increase of load. The SHG efficiency is found to be 2 times than that of KDP.

References

- [1] R. Pepinsky, Y. Okaya., D.P Eastman, Mitsui.T, Phys. Rev., **107**, 1538 (1957).
- [2] Pepinsky.R, Vedam.K and Okaya.Y, Phys. Rev. **110**, 1309 (1958).
- [3] Deepthy .A and Bhat H.L, J. Cryst. Growth., **226**, 287 (2001).
- [4] Hoshino.S, Okaya.Y and Pepinsky.R, Phys. Rev., **115**, 323 (1959).
- [5] Hoshino.S, Mitsui.T, Jona .F and Pepinsky.R, Phys. Rev. **107**, 1255 (1957).

-
- [6] Pares.S, Cohen-Addad .C, Sieker .L.C, Neuburger.M and Douce.R, Acta Cryst., **D51**, 1041 (1995).
- [7] Mohana Rao .J.K and Natarajan.S, Acta Cryst. **B36**, 1058 (1980).
- [8] Freeman.H.C and Guss.J.M, Acta Cryst. **B28**, 2090 (1972).
- [9] Averbuch-Pouchot.M.T, Durif .A and Guitel.J.C, Acta Cryst., **C44**, 99-102 (1988).
- [10] J. Baran , Drozd .M, Pietraszko .A, Trzebiatowska .M, and Ratajczak . H J. Polish.Chem., **77**, 1561 (2003).
- [11] Subha Nandhini M., Natarajan S., Sivakumar K., B. Varghese Acta Cryst., **C57**, 1149 (2001).
- [12] Wenwei Ge, Huaijin Zhang, Jiyang Wang , Donggang Ran, Shangquian Sun, Hairui Xia, Junhai Liu, Xiangang Xu, Xiaobo Hu, and Minhua Jiyang, J.Cryst.Growth. **282**, 320 (2005).
- [13] Krishnakumar.V and Nagalakshmi .R, Spectrochim. Acta A., **61**, 499 (2005).
- [14] Krishnakumar.V and John Xavier.R, Spectrochim. Acta A ., **60**, 709 (2004).
- [15] Chawla .A.K, Kaur.D, and Chandra.R, Opt. Mater., **29**,995 (2007).
- [16] Eya .D.D.O, Ekpunobi.A.J, and Okeke .C.E, Acad. Open Internet J. 2006, 17
- [17] Denton.R.E, Campbell.R.D and Tomlin .S.G, J. Phys., **D5**, 852-863 (1972).
- [18] Ashour.A, El-Kadry .N, and Mahmoud.S.A, Thin Solid Films., **269** ,117-120 (1995)
- [19] Pricilla Jeyakumari A., Ramajothi J. and Dhanuskodi. S, Journal of Crystal Growth, **269**, 558 (2004).
- [20] Rao K.V. and Smakula A, J. Appl. Phys. **36**, 2031 (1965).
- [21] Xavier, F. P, Inigo, A. R., Goldsmith. G. J, Parphyrins, Journal of Porphyrins and Phthalocyanines **3**, 679-686 (1999).
- [22] Joshi, V. N. Photoconductivity; Marcel Dekker: New York, 1990.
- [23] Kityk.V, Marciniak.B, and Mefleh.A, J. Phys., D **34**, 1-4 (2001).
- [24] Susmita Karan, Sen Gupta .S.P, Mat. Scie. Engg A., **398**, 198 -203 (2005)
- [25] Banwari Lal, et al., Mat. Chem. Phys., **85**, 353-365 (2004).
- [26] Vineeta Gupta, et al., Mat. Chem. Phys., **89**, 64-71 (2005).